SPS/ABM

LEP Note 397
21.06.82

POSSIBLE USES OF SYNCHROTRON RADIATION FOR ELECTRON BEAM PROFILE MONITORING IN LEP AND SPS

J. Bosser, R. Coïsson, A. Hofmann, F. Méot

Abstract

We describe various methods of using the synchrotron radiation in the visible or X-ray range emitted by electrons and positrons in LEP and its injector SPS, to monitor the beam profile. We also make some specific proposals for new monitors and for the use of some existing monitors.

Introduction

Synchrotron radiation (SR) is widely used to observe the transverse beam dimensions and profile in electron storage rings, using either visible light and a telescope or X-rays and a pinhole camera.

For a survey of these methods, see ref. 1. A description of specific examples (PEP and SPS) is given in ref 2. A discussion of the geometrical optics of the observation of SR is given in ref. 3, while the limitations imposed by diffraction are discussed in ref. 4.

This report is intended to describe various ways in which SR (or related phenomena) could be used specifically on LEP, and its injector SPS, to monitor beam size and profile (and possibly other data, such as intensities and bunch length), and some specific proposals are made, including the possible use of existing SPS monitors (ref. 2b), and observations in transfer lines.

Although the basic physics of SR emission has in fact been reviewed in connection with its specific application to LEP (ref.5 to which the reader may refer) a brief summary is included of those formulae which give the intensity of SR at low frequencies and large angles and its angular aperture.

The main goal will be to determine, for each method, the order of magnitude of the light power on the detector and the resolution limits.

For practical reasons, considerations relate essentially to radiation which can travel in air, i.e. visible ($\lambda \gg 2000$ Å) or X-rays ($\lambda \ll 3$ Å), and for which imaging and detection technologies are available. The 'low frequency' approximations of SR will usually apply to both visible light and X-ray of $\lambda \simeq 1$ Å, as in most cases the 'critical wavelength' will be lower than 1 Å.

The plan for the following chapters is as follows. Part I is of general interest while Part II is more specific.

PART I

2) Limits to imaging: (a) Diffraction, (b) Depth of field,

3) SR at low frequencies and wide angles: (a) bending magnets, (b) 'short' magnets, (c) undulators, (d) Compton scattering,

PART II

4) SR from bending magnets: X-rays,

5) SR from bending magnets: visible light,

6a) SR from 'short' magnets and undulators,

6b) Possible use of the SPS undulator,

7) SR from quadrupoles (beam position and sizes),

8) SR from beam-beam interaction,

9) Beam scanning by Compton scattering,

10) Transfer lines,

11) Conclusion.

The symbols used are listed in table 1, while table 2 shows the range of parameters which we consider for LEP and SPS.

Table 1

Symbols used

m_o	electron mass	$m_o = 9{,}108 \times 10^{-31}$ kg
e	electron charge	$e = -1{,}602 \times 10^{-19}$ As
B	magnetic field in Tesla	
c	speed of light	$c = 2{,}998 \times 10^{8}$ ms^{-1}
E_o	energy at rest	$E_o = m_o c^2 = 0{,}511$ MeV $= 0{,}511 \times 10^{-3}$ GeV
v	particle speed	$\beta = v/c$
ν	frequency	
ω	angular frequency	$\omega = 2\pi\nu$
n	number of electrons per second	
Ω	solid angle	
I	electron beam intensity in A	
p	number of electrons circulating in the accelerator	
λ	wavelength	$\lambda = c/\nu$
r_o	electron radius	$r_o = 2{,}818 \times 10^{-15}$ m $= \frac{1}{4\pi\varepsilon_o} \frac{e^2}{m_o c^2}$

Table 2

	SPS	LEP
E particle energy: GeV	$3{,}5 \leq E \leq 22$	$22 \leq E \leq 52$
$\gamma = E/E_o$	$6850 \leq \gamma \leq 43{,}000$	$43{,}000 \leq \gamma \leq 101{,}760$
ρ radius of curvature m	741	3104
Critical angular frequency $\omega_c = \frac{3c\gamma^3}{\rho}$	$3{,}904 \cdot 10^{17} \leq \omega_c \leq 9{,}657 \cdot 10^{19}$	$2{,}305 \cdot 10^{9} \leq \omega_c \leq 3{,}055 \cdot 10^{20}$
Critical energy W_c (eV)	$2{,}6 \cdot 10^{2} \leq W_c \leq 6{,}36 \cdot 10^{4}$	$1{,}52 \cdot 10^{4} \leq W_c \leq 2{,}01 \cdot 10^{5}$

PART 1

2. Limits to imaging

As the radiation emitted by the whole beam is the incoherent superimposition of that emitted by each electron, the transverse distribution of intensity (power per unit surface) at the source is proportional to the current density in the beam.

The source also has a longitudinal distribution, which is given by the instantaneous intensity emitted in the direction of the observer as a function of the longitudinal co-ordinate, along each electron's motion.

The finite aperture of the radiation and its longitudinal extension imply that the image formed by a lens or telescope will not be an exact copy of the transverse distribution of the source, but will be blurred by the effect of diffraction, the limited depth of field and the orbit curvature (in the case of bending magnet SR). The transfer function of the imaging tube itself will also have to be taken into account. Hereafter all the errors will be referred to the source.

(a) Diffraction

The fact that the propagation of light obeys a wave equation and the angle of emission is limited implies that we can consider that the ideal image of a source is being convoluted by the Fourier transform of the emitted radiation angular distribution $f(\theta, \varphi)$. If the angular aperture of that band of radiation (wavelength λ) detected by the image-forming device is θ_a, the image of a point (point-spread function or Green's function) will be a distribution of intensity whose width corresponds, at source level, to

$$d = \lambda/\theta_a \qquad (1)$$

The exact form of this distribution for some important cases (bending magnet, undulator, etc..) has been numerically calculated in ref. 4.

For a (e.g. horizontal) beam distribution which is approximately gaussian, we can roughly estimate that the observed width $\sigma_{x\,obs}$ will be

$$\sigma_{x\,obs} \simeq \left(\sigma_x^2 + \lambda^2/\theta_a^2\right)^{1/2} \qquad (2)$$

where σ_x is the actual source width.

(b) Depth of field

Another cause of blurring is the limited depth of field and the non-zero longitudinal extension of the source.

A single electron would be a line source of intensity $\ell(z)$ (with full length L); if the optical image-forming device is focused at the centre of the longitudinal distribution $\ell(z)$, a single-electron image would be given by the contribution of each point z' of the line source (fig. 1).

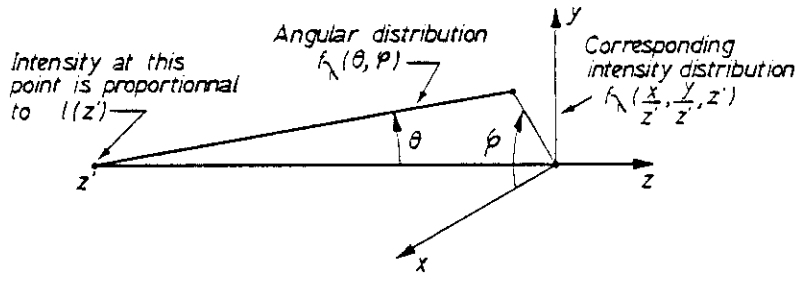

fig. 1

then the image of a beam is convoluted by the point-spread function

$$g(x,y) = \int \ell(z')\, f_\lambda\left(\frac{x}{z'}, \frac{y}{z'}, z'\right) dz' \qquad (3)$$

and therefore depends on the angular distribution $f_\lambda(\theta, \varphi)$ or $f_\lambda(\theta_x, \theta_y)$ and on the length L of the observed trajectory, which may, for example in a bending magnet, depend also on the angular distribution f_λ and on λ.

For an order of magnitude estimate, if still θ_c is the effective aperture of f_λ, the width of the point-spread function is

$$\delta \simeq \frac{1}{4} L \theta_c \qquad (4)$$

(c) Distortion caused by orbit curvature

If the trajectory where the beam is observed is curved, a distortion results owing to lateral displacement with z. For a uniform magnet a simple scheme is indicated in fig. 2.

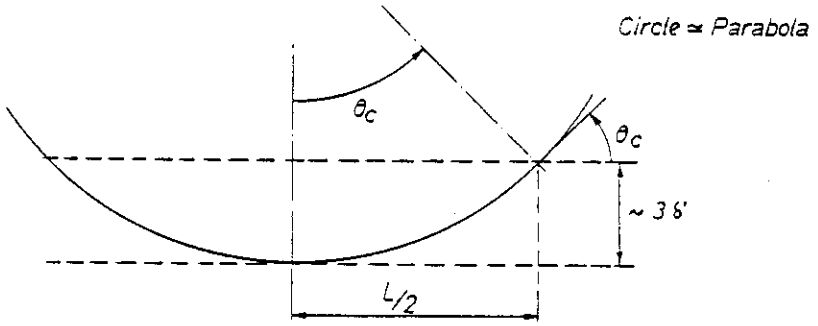

Fig. 2

which shows that the order of magnitude of the spread of a point image due to this effect is

$$\delta' \simeq \frac{1}{6} \rho \theta_c^2 = \frac{1}{2} L \theta_c \qquad (5)$$

Note. Problems of aberration (such as chromatic, etc.) and tolerances of optical systems are not discussed here, but although they can be kept at a value lower than the other - more fundamental - limitations, they will have to be kept in mind in practice and require a careful optical design. In conclusion, the ideal image is convoluted with two known functions: one

of width d and another of width δ (and possibly a third one δ').

The resolution limits d and δ do not mean that the uncertainty of the measurements of beam size cannot be lower than $d+\delta$ or $(d^2+\delta^2)^{1/2}$, but depending on the width of profiles and signal/noise ratios, a deconvolution can reduce the uncertainty in the measurement to 1/2 to 1/5 of that value.

(d) Optics

Concerning the optical system, large distances are usually involved. Thus apart from the problem of aberrations, the tolerances are tight. Moreover mechanical precautions should be taken according to the heating and vibrations. On the other hand, the image-sensor must have a definition (lines per mm) depending on the optical magnification.

3. Some results of the basic theory of synchrotron radiation and related phenomena.

3.1 General procedure

The radiation emitted by an ultrarelativistic ($\gamma \gg 1$) electron moving in a magnetic field B which is perpendicular to the plane of the orbit (fig.3) is given by Liénard's formula (6). It gives the field components E_σ (parallel to the orbit plane) and E_π (perpendicular to it) in the approximation of small instantaneous angle θ between the velocity $\vec{v}$ of the particle and the direction of observation for the two-field components:

$$E_\sigma(r,t) = \frac{4 c r_0 \gamma^3 B(t')}{r} \cdot \frac{(1-\gamma^2\theta^2\cos 2\phi)}{(1+\gamma^2\theta^2)^3} \qquad (6)$$

$$E_\pi(r,t) = -\frac{4 c r_0 \gamma^3 B(t')}{r} \cdot \frac{\gamma^2\theta^2 \sin 2\phi}{(1+\gamma^2\theta^2)^3}$$

and for the absolute value

$$\left|E(r,t)\right| = \frac{4 c r_0 \gamma^3 B(t')}{r(1+\gamma^2\theta^2)^2} \cdot \left(1 - \frac{4\gamma^2\theta^2\cos^2\phi}{(1+\gamma^2\theta^2)^2}\right)^{1/2}$$

Here r is the distance between the particle and the observation point and t' is the time of emission of a photon which arrives at the observation point at the time t

$$t' = t - \frac{r}{c} \quad ; \quad \frac{dt}{dt'} = 1 + \frac{1}{c}\frac{dr}{dt} = 1 - \frac{v}{c}\cos\theta \simeq \frac{1+\gamma^2\theta^2}{2\gamma^2} \qquad (7)$$

Furthermore B(t') is the magnetic field at the location of the particle at the time t', r_o is the classical electron radius and the angles φ and θ are explained in fig. 3.

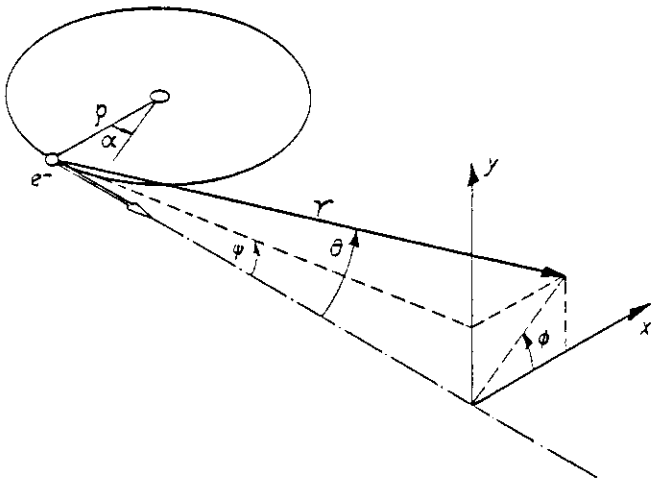

fig. 3 Geometry of the synchrotron radiation emission

The instantaneous power emitted by one electron per unit solid angle in the direction θ to the observer is

$$\frac{dP}{d\Omega} = \varepsilon_o c r^2 E^2 \frac{1+\gamma^2\theta^2}{2\gamma^2}$$

$$\frac{dP_\sigma}{d\Omega} = \frac{3P_o\gamma^2}{\pi} \cdot \frac{(1-\gamma^2\theta^2\cos 2\phi)^2}{(1+\gamma^2\theta^2)^5} \qquad (8)$$

and

$$\frac{dP_\pi}{d\Omega} = \frac{3P_o\gamma^2}{\pi} \cdot \frac{(\gamma^2\theta^2 \sin 2\phi)^2}{(1+\gamma^2\theta^2)^5}$$

where P_0 is the total radiated power

$$P_0 = \frac{2}{3}\,\frac{c^3 e^2 r_0 B^2 \gamma^2}{m_0 c^2} = \frac{2}{3}\,\frac{c\, r_0\, m_0 c^2 \gamma^4}{\rho^2}$$

with ρ being the radius of curvature.

The total power into each of the two polarisation components is

$$P_\sigma = \frac{7}{8} P_0 \qquad \text{and} \qquad P_\pi = \frac{1}{8} P_0$$

For a whole beam with instantaneous current I the total power radiated per unit length of orbit can be given:

$$\frac{dP_T}{d\gamma} = \frac{2 r_0 m_0 c^2 \gamma^4 I}{3 e \rho^2}$$

To obtain the spectral distribution of the radiation the Fourier transform

$$\widetilde{E}(\omega) = \mathcal{F}\{E(t)\} = \frac{1}{\sqrt{2\pi}} \int E(t)\, e^{-i\omega t}\, dt \qquad (9)$$

is made for the two polarisation components. The spectral distribution of the energy W radiated per unit solid angle in the direction of the observer during one passage of the particle is

$$\frac{d^2 W}{d\Omega\, d\omega} = \varepsilon_0 c r^2 \left| \mathcal{F}\{E(t)\} \right|^2 \qquad (10)$$

In making the Fourier transform (eq. 9) it should be noted that in general the angles θ and φ appearing in the expressions (eq. 6) for E(t) depend on t since the direction of the particle velocity changes. Only if the occurring deflection of the trajectory is small compared to the observation angle θ can this time dependence be ignored, as in the case of 'short' magnet and weak field undulator radiation.

3.2 Uniform magnetic field

The angular aperture of the emitted radiation (eq. 8) is of the order of $\sim 1/\gamma$ (or a few times $1/\gamma$ if we also consider the weak tails which contribute to the low frequency part of the spectrum). For a uniform magnetic field B this means that the main contribution to the radiation seen by an observer originates from a part of the electron trajectory of length

$$L_0 \simeq \frac{2\rho}{\gamma} = \frac{2 m_0 c^2}{e B c} \qquad (11)$$

If B is uniform over more than this length we are dealing with ordinary synchrotron radiation and the observer sees, from each electron, a flash of duration

$$\tau \simeq \frac{4}{3}\frac{\rho}{c\gamma^3} = \frac{2}{\omega_c} \qquad (12)$$

where $\omega_c = \frac{2}{3} c\gamma^2/\rho$ is the 'critical frequency' and $W_c = \hbar\omega_c$ the critical energy which is in practical units

$$W_c\,(\mathrm{Kev}) = 2.22\,\frac{E[\mathrm{Gev}]^3}{\rho[\mathrm{m}]} \simeq 0.665 \cdot B[\mathrm{T}] \cdot E^2[\mathrm{Gev}] \qquad (13)$$

The quantitative spectral angular distribution of the energy radiated per revolution is for ordinary synchrotron radiation (6,7,8)

$$\frac{d^3W}{d\alpha\, d\psi\, d\omega} = \frac{r_0 m_0 c^2}{3\pi^2 c^3}\rho^2\omega^2\left(\frac{1}{\gamma^2}+\psi^2\right)^2\left[K_{\frac{2}{3}}^2(\xi) + \frac{\psi^2}{1/\gamma^2+\psi^2}K_{\frac{1}{3}}^2(\xi)\right]$$

$$\xi = \frac{\rho\omega}{3c}\left(\frac{1}{\gamma^2}+\psi^2\right)^{3/2} \qquad (14)$$

with $K_{2/3}$ and $K_{1/3}$ as modified Bessel functions; ψ is the angle between the direction of observation and the orbit plane (fig. 3) and α is the angle parallel to this plane. The first term in the square brackets gives the σ-mode with the electric field being parallel to the plane of orbit and the second term gives the π-mode having the field perpendicular to this plane.

For large angles $\psi >> 1/\gamma$ we obtain

$$\xi \simeq \frac{\rho\omega}{3c}\psi^3$$

and the expression (eq. 14) becomes independent of energy

$$\frac{d^3W}{d\alpha.d\psi.d\omega} \simeq \frac{r_0 m_0 c^2 \rho^2 \omega^2 \psi^4}{3\pi^2 c^3}\left[K^2_{\frac{2}{3}}(\xi) + K^2_{\frac{1}{3}}(\xi)\right] \qquad (15)$$

From (eq. 15) it is possible to estimate the typical vertical opening angle of the synchrotron radiation at low frequencies $\omega << \omega_c$

$$\psi_c \simeq \frac{1}{\gamma}\left(\frac{\omega_c}{\omega}\right)^{1/3} = \left(\frac{3c}{2\omega\rho}\right)^{1/3} \qquad (16)$$

At this value for ψ and $\omega << \omega_c$ the intensity of the σ-mode in eq. 15 is about one-half of its value at $\psi = 0$ and the π-mode intensity is close to its maximum. By integrating (eq. 14) over all angles we obtain spectrum of the total radiated energy in one turn.

The exact spectrum is : $$\frac{dW}{d\omega} = \frac{W_0}{\omega_c} S\left(\frac{\omega}{\omega_c}\right) \qquad (17)$$

With W_0 as the total energy radiated by one electron in one revolution

$$W_0 = \frac{4\pi r_0 m_0 c^2 \gamma^4}{3\rho}$$

and S the normalised spectral function (ref.9)

$$S\left(\frac{\omega}{\omega_c}\right) = \frac{9\sqrt{3}}{8\pi}\left(\frac{\omega}{\omega_c}\right)\int_{\omega/\omega_c}^{\infty} K_{\frac{5}{3}}\left(\frac{\omega}{\omega_c}\right) d\left(\frac{\omega}{\omega_c}\right) \qquad (18)$$

The number of photons radiated all around the ring by a current I into a relative bandwidth $\frac{\Delta\omega}{\omega}$ is (eq. 10)

$$\frac{dn}{d\omega/\omega} = \frac{16\pi^2 r_0 E.I}{c\,h\,e}\, S\left(\frac{\omega}{\omega_c}\right) = 2.49\cdot 10^{20} E[\mathrm{GeV}]\, I[\mathrm{A}] \qquad (19)$$

with $h = 6.626\cdot 10^{-34}$ J.s = Planck's constant.

The partition of the low frequency part of the spectrum into the two polarisation modes is

$$\frac{dW_\sigma}{d\omega} = \frac{3}{4}\frac{dW}{d\omega}\,, \quad \frac{dW_\pi}{d\omega} = \frac{1}{4}\frac{dW}{d\omega} \quad \text{for } \omega \ll \omega_c$$

For the low energy part of the spectrum it is also possible to approximate this function $S(\frac{\omega}{\omega_c})$ by

$$S\left(\frac{\omega}{\omega_c}\right) \simeq \frac{9}{2.2^{1/3}\,\Gamma\left(\frac{1}{3}\right)}\left(\frac{\omega}{\omega_c}\right)^{1/3} = 1.33\left(\frac{\omega}{\omega_c}\right)^{1/3} \qquad (18')$$

The total power radiated by a current I per unit bending angle α is

$$\frac{dP_I}{d\alpha} = \frac{2\,r\,m_0 c^2 \gamma^4 I}{3\,e\,\rho} = \frac{2\,r_0 E^4 I}{3\,e\,(m_0c^2)^3\,\rho}$$

or in practical units

$$\frac{dP_I[\mathrm{Watt}]}{d\alpha[\mathrm{mrad}]} = 14.1\,\frac{E^4[\mathrm{GeV}]\cdot I[\mathrm{A}]}{\rho[\mathrm{m}]}$$

3.3. 'Short' magnets

If a magnet produces a maximum deflection $\alpha \ll 1/\gamma$ the angular factor in eq. 6 can be considered as constant and the spectral properties of the radiation are determined by the spatial variation of the magnetic field $B(z)$ (ref. 11):

$$\frac{dW_\sigma}{d\Omega\, d\omega} = \frac{c^3 e^2 r_0 \gamma^2}{\pi\, m_0 c^2}\cdot\frac{(1-\gamma^2\theta^2\cos 2\phi)^2}{(1+\gamma^2\theta^2)^4}\cdot\left|\widetilde{B}\left(\frac{\omega(1+\gamma^2\theta^2)}{2\gamma^2}\right)\right|^2$$

$$\frac{d^2W_\pi}{d\Omega\, d\omega} = \frac{c^3 e^2 r_0 \gamma^2}{\pi m_0 c^2} \cdot \frac{(\gamma^2\theta^2 \sin 2\phi)^2}{(1+\gamma^2\theta^2)^4} \cdot \left| \tilde{B}\left(\frac{\omega(1+\gamma^2\theta^2)}{2\gamma^2} \right) \right|^2 \tag{20}$$

$$\frac{d^2W_{tot}}{d\Omega\, d\omega} = \frac{c^3 e^2 r_0 \gamma^2}{\pi m_0 c^2} \frac{1}{(1+\gamma^2\theta^2)^2} \left(1 - \frac{4\gamma^2\theta^2\cos^2\phi}{(1+\gamma^2\theta^2)^2} \right) \left| \tilde{B}\left(\frac{\omega(1+\gamma^2\theta^2)}{2\gamma^2} \right) \right|^2$$

with $\tilde{B}(\omega')$ being the Fourier transformation of the magnetic field.

$$\tilde{B}(\omega') = \frac{1}{\sqrt{2\pi}} \int B(z/c) \exp(-i\omega' z/c)\, d(z/c) .$$

For a magnet made of a single short bump with peak field B_0 and length L such that total bending angle α is small

$$\alpha\gamma \simeq \frac{eB_0 Lc}{m_0 c^2} = K \ll 1 \tag{21}$$

the typical wavelength λ_s of the radiated spectrum is

$$\lambda_s(\theta) \simeq \frac{L}{2\gamma^2}\left(1+\gamma^2\theta^2\right) \tag{22}$$

which is independent of B_0.

At $\theta = 0$ this wavelength $\lambda_s(0)$ is shorter than the critical wavelength of the spectrum radiated by a corresponding uniform magnet.

$$\lambda_c = \frac{2\pi c}{\omega_c} = \frac{4\pi\rho}{3\gamma^3} \simeq \frac{4\pi L}{3\alpha\gamma^3} = \frac{8\pi}{3\alpha\gamma}\lambda_s(0) \gg \lambda_s(\theta)$$

If the observation angle θ is large, $(\theta\gamma \gg 1)$ the 'short' magnet approximation is valid as long as $\alpha \ll \theta$.

As will be seen this means that in some cases of interest to us, like synchrotron radiation from quadrupoles and beam-beam synchrotron radiation, for observation at large angles the 'short' magnet approximation will be valid even if $\alpha > 1/\gamma$.

For $\theta \gg 1/\gamma$ we have

$$\lambda_s(\theta) \simeq \frac{1}{2} L \theta^2$$

which means that the radiation of wavelength λ extends up to an angle

$$\theta_s \simeq \left(\frac{2\lambda}{L}\right)^{1/2} \tag{23}$$

At these large angles $\theta \gg 1/\gamma$ the radiated energy per unit solid angle for the two polarisation directions becomes

$$\frac{dW_\sigma}{d\Omega\, d\omega} \simeq \frac{c^3 e^2 r_0}{\pi m_0 c^2} \left|\tilde{B}\left(\frac{\omega\theta^2}{2}\right)\right|^2 \frac{\cos^2 2\phi}{\gamma^2 \theta^4}$$

$$\frac{dW_\pi}{d\Omega\, d\omega} \simeq \frac{c^3 e^2 r_0}{\pi m_0 c^2} \left|\tilde{B}\left(\frac{\omega\theta^2}{2}\right)\right|^2 \frac{\sin^2 2\phi}{\gamma^2 \theta^4} \tag{24}$$

and decreases with the square of particle energy.

The two polarisation modes have equal intensity and show a four-fold symmetry in ϕ as indicated in fig. 4.

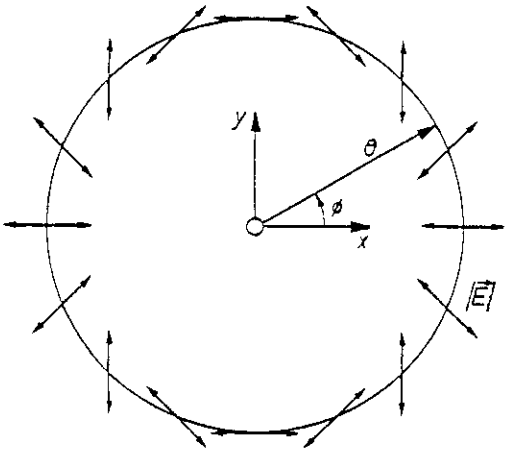

fig. 4 Polarization direction of the synchrotron radiation of a short horizontally deflecting magnet observed at large angle θ.

3.4 Undulators

An undulator (12) consists of a spatially periodic magnetic field in which an electron emits quasi-monochromatic synchrotron radiation. We consider a transverse undulator with a sinuosoidal magnetic field:

$$B(z) = B_0 \sin \frac{2\pi}{\lambda_0} z \tag{25}$$

of total length L with $N = L/\lambda_0$ periods. It emits radiation which, at each angle θ, consists of a narrow band around the wavelength

$$\lambda_1(\theta) = \frac{\lambda_0}{2\gamma^2}\left(1 + \frac{1}{2}K^2 + \gamma^2\theta^2\right) = \frac{2\pi c}{\omega_1} \tag{26}$$

where the 'deflection parameter' K is defined as for a 'short' magnet

$$K = \alpha\gamma = \frac{e B_0 \lambda_0 c}{2\pi m_0 c^2} = 93.4\, B_0[T] \cdot \lambda_0[m] \tag{27}$$

If K<<1 all 'short magnet approximations' apply and the spectrum does not also contain higher harmonics of λ_1. Assuming now that $K \lesssim 1$ the bandwidth at each angle θ is

$$\frac{\Delta\lambda}{\lambda} \simeq \frac{1}{N} = \frac{L}{\lambda_0} \tag{28}$$

The total power radiated into the lowest harmonic is proportional to γ^2

$$P_1 = \frac{r_0 c^3 e^2 B_0^2 \gamma^2}{3 m_0 c^2 \left(1 + \frac{1}{2}K^2\right)^2} \tag{29}$$

(which means that $P_1 \frac{L}{c} \cdot \frac{I}{e}$ is the power emitted by a current I in an undulator of length $L = N\lambda_0$).

The power radiated per unit solid angle is proportional to γ^4

$$\frac{dP_\sigma}{d\Omega} = \frac{3P_1\gamma^2}{\pi\left(1+\frac{1}{2}K^2\right)} \cdot \frac{\left(1-\gamma^2\theta^2\cos 2\phi\right)^2}{\left(1+\gamma^2\theta^2\right)^5}$$

$$\frac{dP_\pi}{d\Omega} = \frac{3P_1\gamma^2}{\pi\left(1+\frac{1}{2}K^2\right)} \cdot \frac{\left(\gamma^2\theta^2\sin 2\phi\right)^2}{\left(1+\gamma^2\theta^2\right)^5} \qquad (30)$$

The spectrum for k<<1 is given by

$$\frac{dP_\sigma/P_1}{d\omega/\omega_{10}} = 3\left(\frac{\omega}{\omega_{10}}\right)\left(\frac{1}{2} - \left(\frac{\omega}{\omega_{10}}\right) + \frac{3}{2}\left(\frac{\omega}{\omega_{10}}\right)^2\right)$$

$$\frac{dP_\pi/P_1}{d\omega/\omega_{10}} = 3\left(\frac{\omega}{\omega_{10}}\right)\left(\frac{1}{2} - \left(\frac{\omega}{\omega_{10}}\right) + \frac{1}{2}\left(\frac{\omega}{\omega_{10}}\right)^2\right) \qquad (31)$$

$$\frac{dP_{tot}/P_1}{d\omega/\omega_{10}} = 3\left(\frac{\omega}{\omega_{10}}\right)\left(1 - 2\left(\frac{\omega}{\omega_{10}}\right) + 2\left(\frac{\omega}{\omega_{10}}\right)^2\right)$$

with $$\omega_{10} = \omega_1(0) = \frac{2\pi c}{\lambda_0} \cdot 2\gamma^2$$

At large observation angles $\gamma^2\theta^2 \gg 1+\frac{1}{2}K^2$ the emitted wavelength is independent of the particle energy

$$\lambda \simeq \frac{\lambda_0\theta^2}{2} \qquad (32)$$

or, the wavelength λ is emitted in a thin conical surface of half opening angle

$$\theta \simeq \left(\frac{2\lambda}{\lambda_0}\right)^{1/2} \qquad (33)$$

At these large angles the radiated power per unit solid angle becomes

$$\frac{dP_\sigma}{d\Omega} \simeq \frac{r_0 c^3 e^2 B_0^2}{\pi m_0 c^2 \left(1+\frac{1}{2}K^2\right)^3} \cdot \frac{\cos^2 2\phi}{\gamma^2\theta^6}$$

$$\frac{dP_\pi}{d\Omega} \simeq \frac{r_0 c^3 e^2 B_0^2}{\pi m_0 c^2 \left(1+\frac{1}{2}K^2\right)^3} \frac{\sin^2 2\phi}{\gamma^2\theta^6} \qquad (34)$$

$$\frac{dP_{tot}}{d\Omega} \simeq \frac{r_0 c^3 e^2 B_0^2}{\pi m_0 c^2 \left(1+\frac{1}{2}K^2\right)^3 \gamma^6\theta^6}$$

The frequency observed at these angles is $\omega_1 << \omega_0$ and the spectrum (eq. 31) is

$$\frac{dP_{tot}/P_1}{d\omega/\omega_{10}} \simeq 3\left(\frac{\omega}{\omega_{10}}\right) \qquad (35)$$

The higher harmonics are negligible at these large angles.

3.5 Compton back-scattering

The scattering of an electromagnetic wave (e.g. laser beam) from an electron (13) is the same phenomenon as undulator radiation, as long as the incident photon energy E_i is small, $E_i \ll m_0 c^2/\gamma$. An electromagnetic wave of wavelength λ and peak magnetic field B is equivalent to an undulator with period length $\lambda_0 = \lambda/2$ and peak magnetic field $B_0 = 2B$. To calculate the total number of back-scattered photons it is useful to describe the reaction with the total cross section

$$\sigma_T = \frac{8\pi}{3} r_0^2 \qquad (36)$$

PART 2

4. SR from bending magnets: X-rays

The SR emitted from bending magnets or any other magnetic structure ('short magnets' and undulators) extends over a very wide range, from the visible (or IR) to very hard X-rays (hundreds of keV). We anticipate the use of either the X-rays of a few Å wavelength or the visible (or near UV: $\sim$ 2000 Å). Although there could be advantages in using the vacuum UV ($\sim$ 500 Å) we think that at present the conditions of having the whole optical system under vacuum are not favourable.

X-ray pinhole camera

The X-ray image seen through a pinhole is a common method of observation of an electron beam (ref.14). In the case of LEP, a major complication is the fact that a great part of the radiation is made of very hard X-rays, for which the attenuation of a sheet of any material (a fraction of a mm thickness) would be low, giving then very low contrast on the image.

A possible method would be to work with the monochromatic (a few Å) radiation Bragg-reflected by a crystal (if necessary with small oscillations of the crystal).

With usual sources, the imaging through a pinhole can be represented (in one dimension, say x) by a (two-dimensional) phase space diagram x,x', see fig. 5.

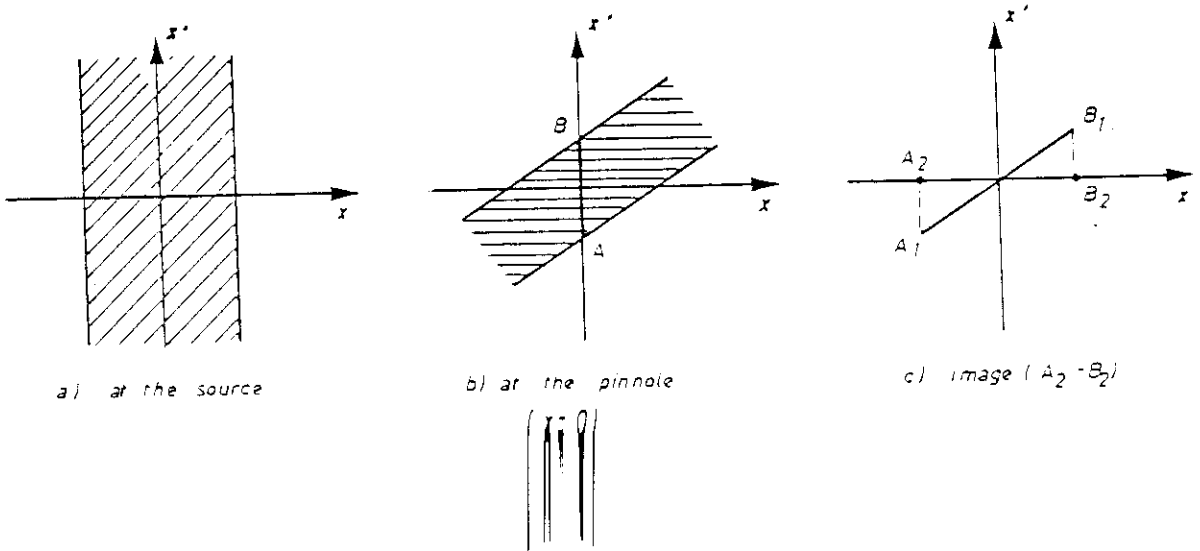

a) at the source b) at the pinhole c) image (A_2 - B_2)

For simplicity, we may consider the pinhole as accepting a well defined angular distribution. If at source level phase space the distribution is given as in a), then after travelling from source to pinhole the phase space diagram is as in b). The pinhole transfers only the fraction given by the line BA which is transformed to B_1A_1 at the image detector. The image seen is represented by the segment A_2B_2.

If the source is isotropic (fig. 5a): the phase space distribution of the source is symmetrical with respect to translation of x'), the 'slice' AB is, apart from a scale factor, equal to the x distribution of the source. In the case of synchrotron radiation sources the phase space diagram is more complex since it is the convolution of the electron beam phase space distribution with the SR angular distribution. This is shown in fig. 6.

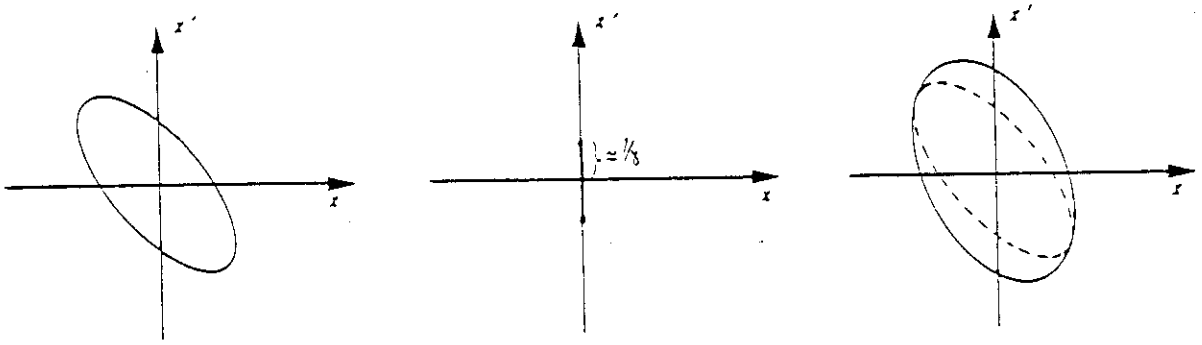

a) electron distrib. b) angular distrib. from a sigle electron c) phase space distrib. of radiation emitted at the source (convolution of a) with b))

fig. 6

Then the imaging process can be represented as in fig. 7.

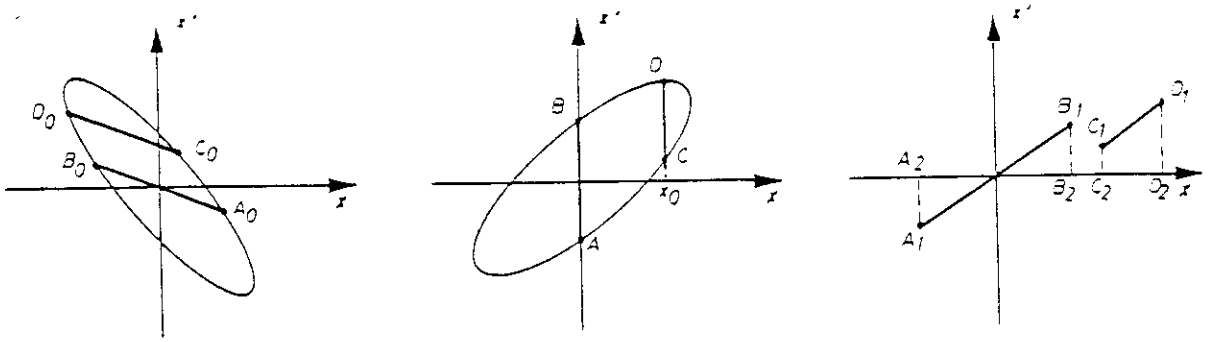

a) at the source (A_1B_1 represents the retro projection of AB onto the source) b) at the pinhole ($x = 0$ or $x = x_0$) c) image (A_2B_2 or C_2D_2)

fig. 7

From this we see that:

1) The image (A_2 B_2) does not represent the spatial distribution of the source but rather the cross-section A_o B_o (fig. 7a) of the phase space of the radiation at the source. Only in particular cases (e.g. angular spread of beam $\ll 1/\gamma$) A_o B_o is approximately proportional to the source spatial distribution.

2) The image depends on the position of the pinhole ($x=0$ or $x=x_o$ in fig. 7b)), or the relative position of the beam.

By scanning the position of the pinhole and detecting the image as a function of the pinhole position, a complete reconstruction of the source (position and angular distribution) could be made by suitable numerical treatment, at least if the electron distribution is gaussian and the angular distribution of SR known. If the distribution is not well known a priori and if the beam position moves in time, the image obtained with a fixed pinhole would change. In this case the scanning pinhole would be an advantage. (A simpler version of monitor could be a pinhole with servo-mechanism to lock the pinhole at maximum SR intensity).

For a 10 μm pinhole diameter and similar resolution on the image, each picture element would receive a fraction of about 10^{-4} of the radiation reflected by the crystal and this intensity is largely sufficient.

For the horizontal dimension, the phase diagram x,x' would look rather like:

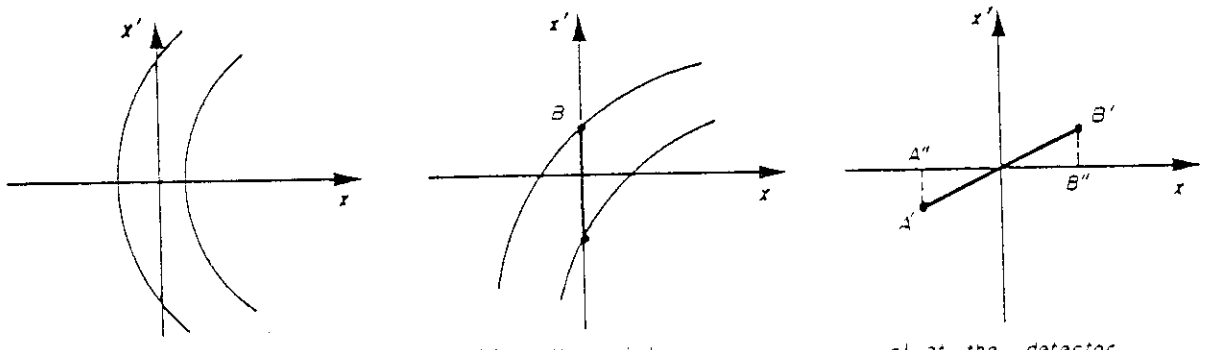

a) at the source b) at the pinhole c) at the detector (A"B": image)

fig. 8

As the opening angle $1/\gamma$ is << 1, the curvature of the distribution can be neglected and the image is independent of the pinhole position. A possible layout may be that given in fig. 9.

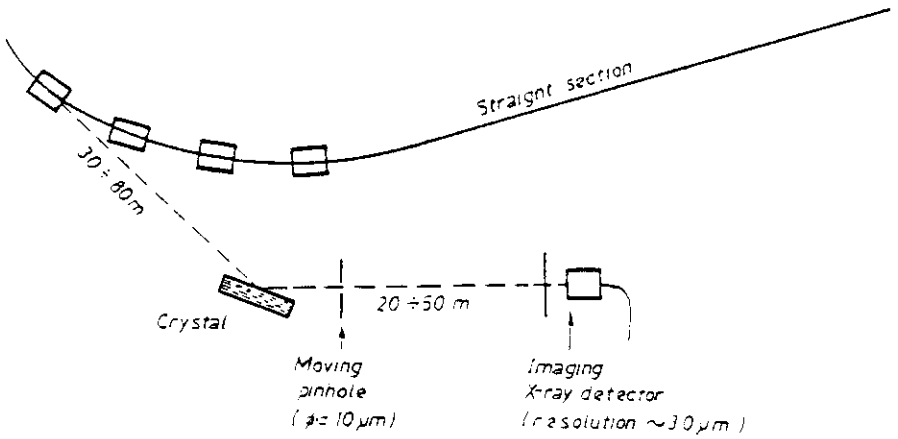

fig. 9

5. Visible SR from bending magnets

We imagine that we observe SR from a bending magnet through a telescope, collecting, say, the light in the band 2000 to 3000 Å (the lowest wavelengths accessible in air, to minimize diffraction and at the same time avoid having the whole apparatus in vacuo).

The effective depth (length) of the source at wavelength λ depends on the opening angle θ_c and the horizontal angle θ_o collected by the lens (fig. 10):

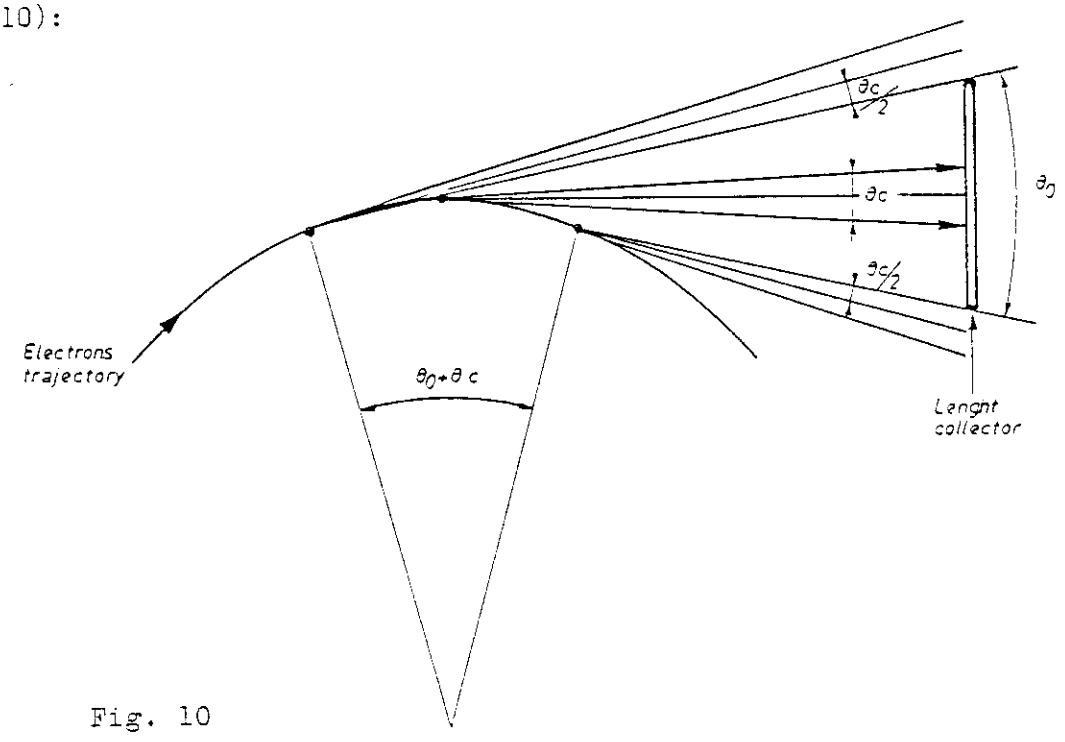

Fig. 10

$$L \simeq 2\rho\left(\theta_c^2 + \theta_0^2\right)^{1/2} \tag{37}$$

while the angular aperture is (eq. 16)

$$\theta_c \simeq \left(\frac{\lambda}{2\rho}\right)^{1/3} \tag{38}$$

in the vertical plane, while

$$\theta_H = \left(\theta_c^2 + \theta_0^2\right)^{1/2} \tag{39}$$

in the horizontal plane.

Then in the vertical plane we have for the effect of diffraction and depth of field:

$$d \simeq \frac{\lambda}{\theta_c} = 2^{1/3}\rho^{1/3}\lambda^{2/3} \tag{40}$$

$$\delta \simeq \frac{1}{4}L\theta_c \simeq \frac{1}{2}\rho\theta_c^2 = 2^{-5/2}\rho^{1/3}\lambda^{2/3} \tag{41}$$

We see that these effects are proportional to each other and independent of energy.

In the horizontal plane:

$$d \simeq \frac{\lambda}{\theta_c + \theta_0} \tag{42}$$

$$\delta \simeq \frac{1}{2}\rho\left(\theta_c + \theta_0\right)^2 \tag{43}$$

When θ is increased d decreases but δ is increased; the optimum case is $\theta_0 \sim \theta_c$ in which $d \sim \delta$:

$$d \simeq \delta \simeq 2^{-2/3}\rho^{1/3}\lambda^{2/3} \tag{44}$$

Also, in the horizontal plane we have a third blurring effect which is distortion (eq. 5):

$$\delta' \simeq \frac{1}{6}\rho\theta_u^2 \simeq \frac{1}{3}\lambda^{1/3}\rho^{1/3}\lambda^{2/3} \qquad (45)$$

in the case $\theta_0 \simeq \theta_c$

In LEP, $\rho \sim 3 \cdot 10^6$ mm, then $d \simeq \delta \simeq 0,5$ mm
In SPS, $\rho \sim 0,75 \cdot 10^6$ mm, then $d \simeq \delta \simeq 0,3$ mm

The intensity in the 2000-3000 Å band, collected over the $2\,\theta_c^2$ solid angle, is of the order of a few μW.

fig. 11a Synchrotron light angular distribution at SPS (e^+, e^-)

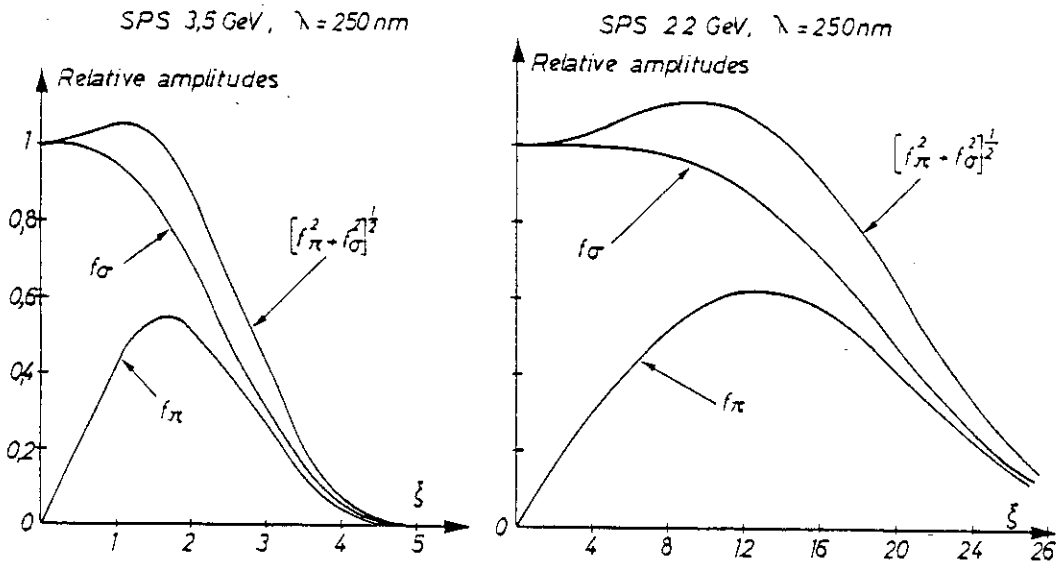

fig. 11b Diffraction pattern at SPS (e^+, e^-)

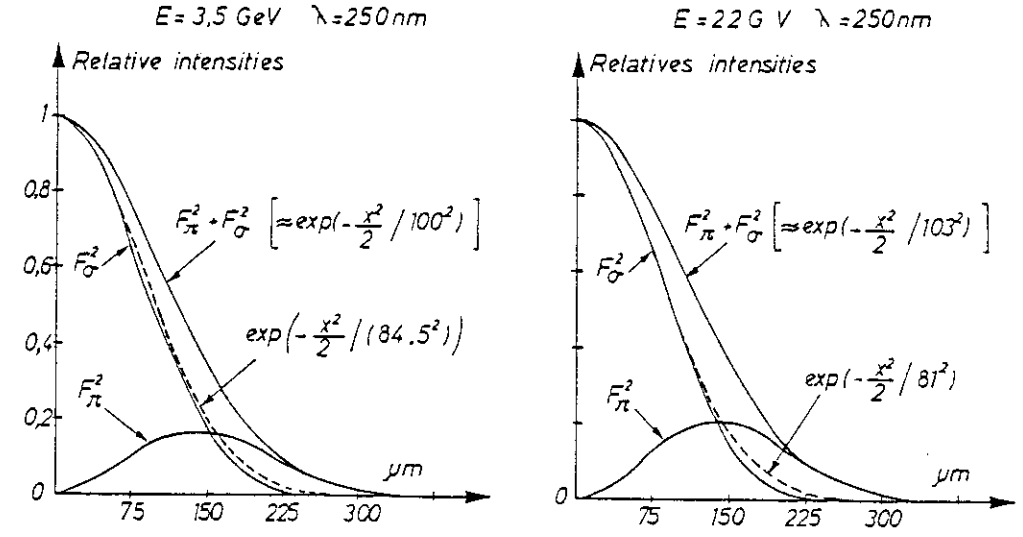

fig. 12 a Angular distribution of synchrotron radiation at LEP

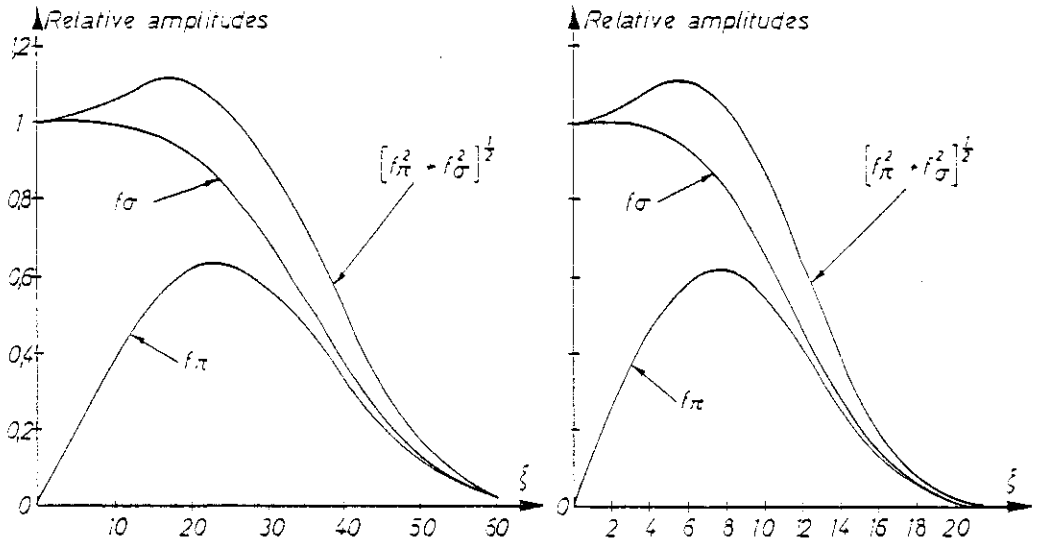

fig. 12 b Diffraction pattern LEP (E = 22 to 30 GeV) for λ = 250 nm

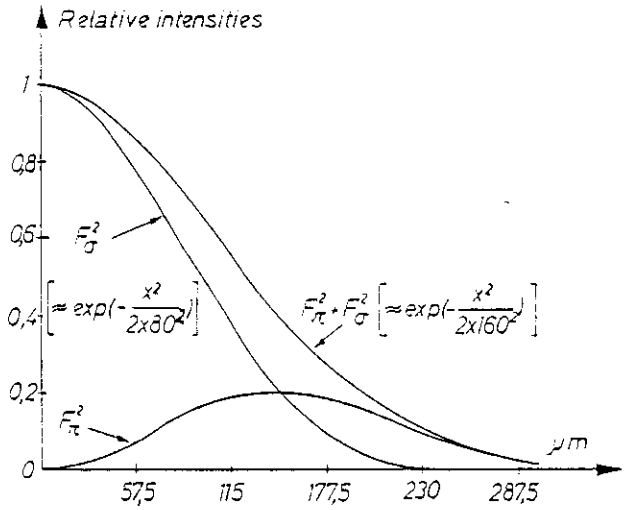

Conclusion

The light intensity is quite sufficient and has the advantage of being independent of energy. However the resolution even with a deconvolution could be of the order of 0.2 ÷ 0.5 mm. This is just enough to resolve the horizontal beam profile but marginal for the vertical profile. Results from numerous calculations of angular distribution and diffraction patterns for SPS and LEP are given in fig. 11 and 12.

6a. SR from 'short' magnets or undulators

As (eq. 23) the opening angle corresponding to a given wavelength is larger than in a bending magnet, we can expect a better resolution with a 'short' magnet (or an undulator).

If L is the length of the magnet (producing a deflection $\alpha << 1/\gamma$), we have from eq. 24 ($\lambda_1 << \lambda$):

$$\theta_s \simeq L^{-1/2} \lambda^{1/2} \tag{46}$$

then (eq. 1 and 4)

$$d \simeq \frac{\lambda}{\theta_c} = L^{1/2} \lambda^{1/2} \tag{47}$$

$$\delta \simeq \frac{1}{4} L \theta_c = \frac{1}{4} L^{1/2} \lambda^{1/2} \tag{48}$$

By analogy for an undulator of period λ_0 and N periods (from eq.33)

$$\theta_s \simeq \lambda_0^{-1/2} \lambda^{1/2} 2^{1/2} \tag{49}$$

$$d \simeq \frac{1}{\sqrt{2}} \lambda_0^{1/2} \lambda^{1/2} \tag{50}$$

$$\delta \simeq \frac{1}{2\sqrt{2}} N \lambda_0^{1/2} \lambda^{1/2} \tag{51}$$

in particular for N = 2 we have δ = d. For 'N = 1/2' we have the preceding case (eq. 47 and 48).

We note that, as for a 'uniform' magnet, the effects of diffraction and depth of field are proportional to each other here, too.

With a 'short' magnet of length L = 10 cm and for $\lambda = 0.2 \cdot 10^{-6}$ m we have, for any machine and any energy: $\mathcal{L} \simeq 0.14$ mm; $\delta \simeq 0.025$ mm.

For an undulator with N = 2 periods, λ_o = 5 cm and B_o = 1000 G, the resolution is determined by d = δ = 0.07 mm, and the total amount of power radiated at 22 GeV by a 1 mA beam is $\simeq$ 150 mW.

But, as the device is usually installed in a straight section, if for practical reasons, only radiation at large angles is collected (to leave space for the e^+ e^- beam) its power is not only much lower but it is proportional to $1/\gamma^2$ (eq. 34) and then the intensity varies strongly during the acceleration cycle (unlike in the case of the bending magnet).

For example, if the light is collected outside an angle θ_o = 0.25 mrd (a hole of 1 cm at 20 m), the 'short' magnet above gives in the wavelength range 2000 Å - 2500 Å, and for B_o = 1000 G:

$$W \simeq 13 \text{ mW}$$

and for the undulator, at wavelength above $\lambda(\theta_o)$:

$$W \simeq 25 \ \mu W$$

for e^+, e^- beam of $\simeq$ 1 mA at 22 GeV.

6b. Possible utilisation of the SPS undulator for $e - \bar{e}$

An undulator has been installed in SPS to observe the transverse distribution of proton and antiproton beams stored at 270 GeV (ref.15a.)

It has $\lambda_u = 8.8$ cm, $\beta_o = 3300$ G

If we detect radiation from 2000 to 3000 Å, the light observed will come out of the undulator along the surface of a cone 2.13 mrad $< \vartheta <$ 2.38 mrad, independent of beam energy. The total power in this case is obtained by integrating eq. 35 from 2000 to 2500 Å

$$W(\Delta\lambda) \simeq 8.44 \cdot \frac{I}{\gamma^2} \simeq \begin{cases} \text{180 nW at 3.5 GeV} \\ \text{4.5 nW at 22 GeV} \end{cases}$$

for e^+, e^- beams of current $I \simeq 1$ mA.

Each polarisation is quite sufficient for detection with an ISIT type TV camera.

The resolution is determined by

$$d \simeq \lambda/\theta_s \simeq 0.1 \text{ mm}$$

$$\delta \simeq (1/4) L \theta_s \simeq 0.2 \text{ mm}$$

Care should be given when we consider a bending magnet emitting 1 μW at 3.4 GeV and more so at 22 GeV.

7. SR from quadrupoles

The SR emitted by a charged particle in a quadrupole magnet depends on its transverse (x,y) position as the magnetic field depends on x,y (fig.13),

$$\vec{B} = k\left(y\,\hat{x} + x\,\hat{y}\right) \qquad \text{(vert. focusing)} \qquad (52)$$

where $\hat{x}$ and $\hat{y}$ are the unit vectors in the x and y directions.

Therefore, the radiation emitted by the whole beam (either total intensity or the visible light intensity) will depend on the beam size and the position of its centre, and then it could be used to monitor these parameters. If the beam current density distribution is

$$J(x,y) = \frac{I}{2\pi\sigma_x\sigma_y} \exp - \left[\frac{(x-x_0)^2}{2\sigma_x^2} + \frac{(y-y_0)^2}{2\sigma_y^2} \right] \tag{53}$$

the total power emitted in the field (eq. 52) (neglecting the change in field due to the curvature of the trajectory) is

$$W = \frac{2}{3} \frac{e^3 I \gamma^2 k^2 L}{4\pi\varepsilon_0 m^2 c^2} \left(x_0^2 + y_0^2 + \sigma_x^2 + \sigma_y^2 \right) \tag{54}$$

If, instead of collecting all the radiation, only the power in a narrow band in the visible (low frequency) range is measured, through a mirror with a hole subtending an angle θ_0 from the source, it can be shown that (ref.15 b.).

$$\frac{dW}{d\lambda/\lambda}(\theta > \theta_0) = \int_{\theta_0}^{\infty} \frac{dW}{d\Omega\, d\lambda/\lambda} = M F \left(\frac{\theta_1}{\theta_0} \right) \frac{I}{\gamma^2} \frac{L^3}{\lambda^2} k^2 \left(x_0^2 + y_0^2 + \sigma_x^2 + \sigma_y^2 \right) \tag{55}$$

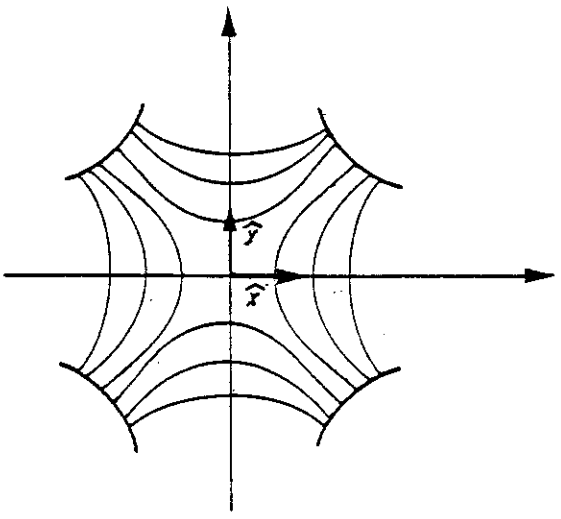

fig. 13

where $\theta_1 = \left(\frac{2\lambda}{L}\right)^{1/2}$ is the opening angle of radiation of wavelength λ, and

$M = \frac{e^3}{16\pi\varepsilon_0 m^2 c^2} \simeq 4\cdot 10^{-4}$ MKS for electrons and

$F(\theta_1/\theta_2)$ is an expression (see ref. 15) which for $\theta_1 \simeq \theta_0$ is $\simeq 1$ and is $\simeq \frac{1}{\pi}\frac{\theta_1^2}{\theta_0^2}$ for $\theta_1 >> \theta_0$.

From eq. 54 and 55 we see that the integrated power or the visible light power observed at large angles is proportional to $x_0^2 + y_0^2 + \sigma_x^2 + \sigma_y^2$.

By feeding some of the quadrupole (QP) windings with inverted connections it is possible to add a uniform magnetic field δB (horizontal or vertical) equivalent to a small displacement of the QP centre. The emitted light power could be used as a feedback to set the QP centre to the beam centre: in this way the beam centre position would be measured (with an accuracy of the order of 10 μm) and the emitted power would remain only proportional to $\sigma_x^2 + \sigma_y^2$. Moreover, the power at the emitted X-rays, which would give a background in the interaction region, would be minimized.

Further information could be obtained by measuring the polarisation of the visible light.

The polarisation of visible light in the direction defined by angle ϕ around the direction $\theta = 0$ is as indicated in fig. 4.

For a centered circular beam $\sigma_x = \sigma_y$ the emitted light is unpolarised. However for a centered elliptic beam the ratio of the two polarisation components depends on the aspect ratio σ_y/σ_x which can be measured in this way.

To discriminate the light coming from a given quadrupole from that coming from other quadrupoles or other sources (bending magnet, beam-beam radiation), it would be necessary to observe the light with a telescope, through a pinhole at the image of the observed quadrupole (where the image of the other sources would be out of focus and most of it out of the pinhole).

In conclusion, minimization of light intensity would give x_o and y_o, the intensity gives $\sigma_x^2 + \sigma_y^2$, while the polarization ratio gives σ_y / σ_x.

In LEP such detectors (for e^+ and e^-) could be inserted in the straight sections near the interaction points where it is particularly important to monitor beam position and size and where the same device could be used (by changing the focus) to observe the beam-beam SR (see sect. 8 and fig. 14).

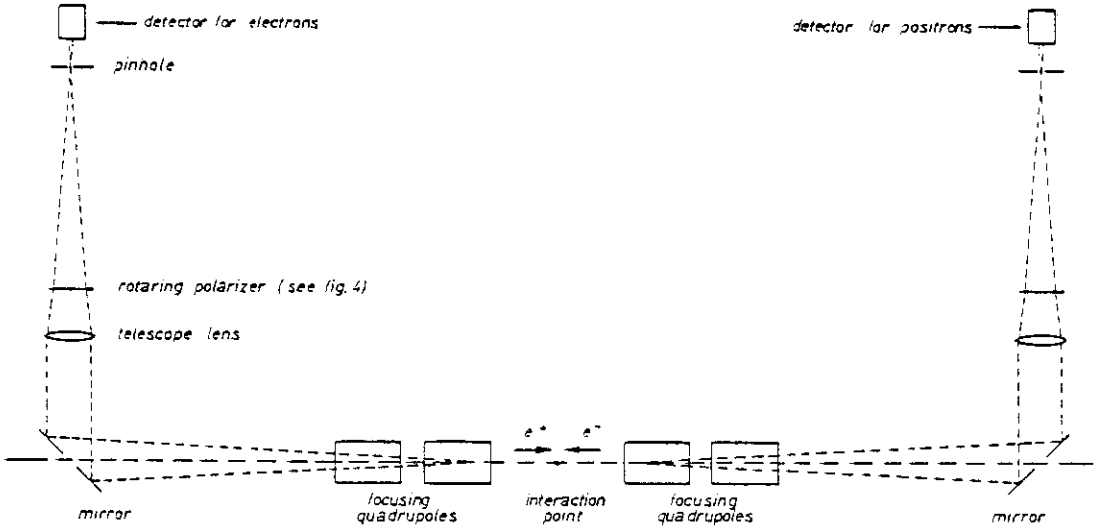

fig. 14

At $\gamma = 10^5$, L = 4 m and k = 50 G/mm, a field modulation $\delta B = 1G$ is equivalent to β's centre position modulation δ_{x_0}, $\delta_{y_0} \sim 20\,\mu m$.

The power collected in a 10% band in the visible with a mirror with a slit of 1 cm at 40 m ($\gamma\theta_0 = 12.5$), is of the order of 1 μW ($\sim 3 \cdot 10^{12}$ photons/s).

With beam sizes of the order of 1 mm and a phase-sensitive detector sensitivity $\sim 10^{-4}$, we can expect 5 to 10 μm resolution for position measurements.

As the radiation background is constant, the modulation measurements would be only slightly affected by the radiation of the environment. Moreover the light could be directed towards an access tunnel so that detectors could be in an area of lower radiation background.

8. Visible beam-beam radiation

In a $e^+ - e^-$ (or $p^+ - p^-$) storage ring, at the interaction point, each particle sees an e.m. field due to the opposite beam and then, after being accelerated, emits radiation.

It has been shown that, when the two beams are perfectly centered, the total power emitted is proportional to luminosity (16).

In LEP, beam-beam radiation has been studied as a possible source of background for high energy physics experiments; the total power emitted at each intersection is of the order of one kW (ref.17,18,20).

The calculation of the spectrum is not simple as the deflection of particles (e^+,e^-) is of the order of $1/\gamma$. Hard X-rays (of the order of one MeV) would be emitted forward (within an angle $\sim 1/\gamma$), while visible light would be observed up to several times $1/\gamma$. With the same argument

as in the case of radiation from quadrupoles, it is easy to show that the amount of visible radiation observed outside a certain angle $\theta_0 >> 1/\gamma$ is proportional to the total power, and polarisation of the radiation emitted by each particle has the distribution shown in fig. 4.

The device described in the preceding section (fig. 14) could be focused either on quadrupoles or on the interaction point. Therefore, the same device could give us monitoring of the luminosity as well as an indication of the relative displacement of the two beams, which could be used for the adjustment of the relative position of the two beams, and then maximisation of the luminosity.

9. Compton scattering

By sending a laser beam on the electron (or positron) bunch, the electrons emit hard X-rays within an angle $\sim 1/\gamma$ around $\theta = 0$ (see sect. 3.5 and ref. 19,20).

If the laser beam is sent towards a direction opposite to the particle bunch and focused to a small spot, the total power of emitted X-rays would be proportional to the particle current density at that point. The laser spot could then be scanned to give the (two-dimensional) transverse distribution. Otherwise, the laser beam can be sent towards a transverse direction and give horizontal or vertical slices of the electron beam profile.

The total power of the emitted X-rays would be measured as a function of laser beam position.

In LEP, for each Compton interaction producing an X-ray photon, an electron is knocked out of the machine. However a sufficient counting rate (obtained with a low power laser) would produce a negligible decrease of beam lifetime.

The smallness of the waste of the focused laser beam (fig. 15) is limited by the diffraction and depth of focus (caused by the finite width of the electron beam and finite angular divergence of the laser beam).

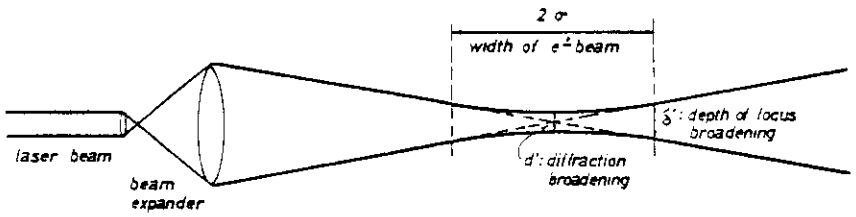

fig. 15

From fig. 15 we see that

$$d' \simeq \frac{\lambda f}{a}$$

$$\delta' \simeq \frac{a}{f}\sigma$$

A compromise must be found between the two resolution limis; for d' $\simeq \delta'$ se have:

$$\frac{a}{f} = \left(\frac{\lambda}{\sigma}\right)^{1/2}$$

In this case

$$d' \simeq \delta' \simeq (\lambda\sigma)^{1/2}$$

In a transverse measurement for $\sigma_x \simeq 3$ mm and $\lambda = 0.5$ μm, the resolution limit is $\alpha' + \sigma' \simeq 80$ μm, while in a head-on measurement with $\sigma_z \simeq 1$ cm, $\alpha' + \sigma' \simeq 140$ μm.

As seen, the resolution is slightly better than that of direct observation of visible SR.

In conclusion, it is probably not worth adding to the above constraint the complication of a laser and that of the mirror scanning system except perhaps if the laser is already there for the measurements of polarisation.

10. Transfer lines

In transfer lines (CPS to SPS and SPS to LEP) though electron-positron beams circulate only once in a machine cycle the collected radiation energy is sufficient for the display of profiles. In the case of bending dipoles general formulae could be used by taking $\theta = 0$ and by considering X-ray factors. The total energy collected is not strong enough to destroy detectors or optics.

Taking TT70 as an example, some magnets give a beam deflection of about 50 mrad which allows easy separation of electron bunches and light beam at about 1 m distance. An X-ray image detector can be used without intermediary optics as the image enlargement is negligible. Therefore a detector for X and Y profiles could be foreseen in any transfer line.

References

1. A. Hofmann, Electron and proton beam diagnostics with SR. IEEE Trans. NS 28-3 (June 1981).

2a. A.P. Sabersky, Optical beam diagnostics on PEP. IEEE Trans.NS (June 1981).

2b. R. Bossart, J. Bosser, L. Burnod, E. d'Amico, G. Ferioli, J. Mann, F. Méot. Proton beam profile measurements with synchrotron light. CERN/SPS/80-8 (ABM).

3. A.P. Sabersky, The geometry and optics of SR. Part.Accel.5, 199-206, (1973).

4. A. Hofmann, F. Méot. Optical resolution of beam cross-section measurements by means of synchrotron radiation. CERN/ISR-TH/82-04.

5. A. Hofmann, Synchrotron radiation from the large electron-positron storage ring LEP. Phys.Rep., 64, 253-281 (1980).

6. J.D. Jackson, Classical electrodynamics. J. Wiley (1962).

7. D.D. Ivanenko, A.A. Sokolov. Doklady Akad.Nauk (SSSR) 59,1551 (1948).

8. J. Schwinger. On the classical radiation of accelerated electrons. Phys.Rev. 75, (1949), 1912.

9. M. Sands. The physics of electron storage rings. SLAC 121 (1970).

10. European synchrotron radiation facility, Suppl. II. The machine. Ed. D.J. Thomson, M.W. Poole. European Scientific Foundation . Strasbourg (1979).

11. R. Coïsson. Angular-spectral distribution and polarisation of synchrotron radiation from a 'short magnet'. Phys.Rev.A20, 524-528 (1979).

12. D.F. Alferov, Yu. A. Bashmakov, E.G. Bessonov. Synchrotron radiation. Lebedev Phys. Inst.Series 80, ed. N.G. Basov, New York Consultants Bureau, 97 (1976).

13. R.H. Milburn, Phys.Rev. Letters 10, (1963),75.

14. A. Hofmann, K.W. Robinson. Measurement of cross section of a high energy electron beam by means of the X-ray portion of the synchrotron radiation. IEEE Trans.on Nucl.Sci. NS, 18, 937 (1971).

15a. F. Méot, Mesure de profils par rayonnement ondulateur des faisceaux de protons et d'antiprotons, CERN/SPS/81-21 (ABM).

15b. R. Coïsson, Synchrotron radiation from quadrupoles as a beam monitor. CERN LEP Note 328 (1981).

16. A. Hofmann, E. Keil. Synchrotron radiation caused by the field of the other beam. LEP Note 70/86 (1978) and Effects of the beam-beam synchrotron radiation. LEP Note 122 (1978).

17. A.N. Skrinski et al. Proc. Soviet Conf.on Charged Particle Accelerators. (1978).

18. M. Bassetti, M. Gygi-Hanney. Dependance of the beam-beam synchrotron radiation on the transverse dimensions for a Gaussian beam. LEP Note 221 (1980).

19. J. Bosser. F. Méot. Effet Compton au SPS. CERN/SPS/80-17 (ABM).

20. R. Rossmanith, R. Schmidt, Laser diagnostics in high energy accelerators, DESY M-81/24 (1981).